

Anomaly Detection in Skull scanning Images based on Multi-sensor Fusion

Xiaochun Guo¹ and Hashim Ali^{2,*}

¹School of Electronics and Information, Nanchang Institute of Technology, No.901, Yingxiong Street, Nanchang 330044, China

²Department of Computer Science, Abdul Wali Khan University, Mardan 23200, KP, Pakistan

Abstract

INTRODUCTION: Skull bones typically possess complex structures and features. When scanned with ordinary sensors, they are easily affected by noise due to the small difference between abnormal areas and normal tissue.

OBJECTIVES: In order to solve the problem of small differences between abnormal areas and normal tissues, which make them susceptible to noise interference, this paper proposes a multi-sensor fusion based skull scan image anomaly detection method.

METHODS: Firstly, the frequency correction factor is utilized to modify the frequency domain characteristics of the sensor signal during the skull scanning image acquisition process, aiming to enhance signal quality and reduce noise impact during acquisition. Secondly, bilateral filters and discrete wavelet transform are employed to subject the skull scanning image to dual domain decomposition in spatial and transformation domains, aiding in distinguishing between normal and abnormal regions. Subsequently, the low-frequency fusion algorithm guided by filtering and the high-frequency fusion algorithm based on multi-scale morphological gradients are fused, and the fused dual frequency components are merged back into the original spatial domain to retain important details. The fused reconstructed image aids in improving the accuracy of anomaly detection. Finally, a backbone network with an auto encoder structure is established to learn the feature representation of fused images, and an unsupervised deep neural network is employed to establish a detection model for anomaly detection in skull scanning images.

RESULTS: Through experiments, it has been demonstrated that the F1 score approaches 1, the ROC curve closely approaches the upper left corner, and the AUC value approaches 1 after applying the proposed method for anomaly detection in skull scanning images.

CONCLUSION: This algorithm has high sensitivity and low specificity, achieving high detection accuracy and demonstrating good performance.

Keywords: Skull scanning images; Bilateral filter; Double domain decomposition; High and low frequency fusion; Deep neural networks

Received on 19 April 2024, accepted on 11 February 2025, published on 12 March 2025

Copyright © 2025 X. Guo *et al.*, licensed to EAI. This is an open access article distributed under the terms of the [CC BY-NC-SA 4.0](https://creativecommons.org/licenses/by-nc-sa/4.0/), which permits copying, redistributing, remixing, transformation, and building upon the material in any medium so long as the original work is properly cited.

doi: 10.4108/eetpht.11.5828

*Corresponding author. Email: hashimali@awkum.edu.pk

1. Introduction

With the advancement of science and technology, intelligent diagnosis based on medical imaging has become a research hotspot. Skull scanning, as an advanced medical imaging technology, has been widely applied in clinical practice [1,2]. People can use modern

medical technologies such as skull scanning to understand their physical condition and disease situation more accurately and thus develop more scientific and personalized treatment plans [3,4]. Skull scanning can non-invasively detect abnormalities in the cranioskeletal system, providing strong support for early detection, accurate diagnosis, and effective treatment of diseases [5,6].

Skull scanning images mainly include various types such as whole-body skull imaging, local skull plane imaging, skull three-phase imaging, skull tomography imaging, skull SPECT/CT imaging, and F18 positron skull imaging. These images detect abnormal morphology or metabolism of skull tissue through radioactive nuclides, helping doctors accurately evaluate the health status of the skull and bones. The abnormal detection of skull scanning images can identify skull metastases and other lesions early, providing an important basis for treatment [7]. This detection method can identify skull metastatic tumours early and is of great significance for patients with tumours of unknown nature.

Traditional skull scanning image analysis demands doctors to possess rich experience and professional knowledge. However, with the continuous development of image processing technology and machine learning algorithms, anomaly detection methods for skull scanning images will increasingly play a significant role in the medical field [8-9]. Currently, abnormal detection of skull scanning images can be automatically accomplished through machine learning algorithms, partially analyzing the skull scanning images, accurately identifying abnormal parts in the images, improving diagnostic accuracy, and reducing doctors' workload [10]. Moreover, algorithms for medical image processing are continually maturing.

In Ref [11], the authors proposed a CT image segmentation and recognition method based on artificial neural networks and morphology. Segmentation and fusion of CT images were achieved through morphology, and fusion thresholds were improved using means, standard deviation, etc. Artificial neural networks were utilized to classify and recognize parts with malignant tumour markers. This method can effectively reduce the workload of doctors and assist in recognizing malignant tumours to a certain extent. However, morphological fusion was usually conducted at a single scale. When processing images with complex scale features, important information may be lost or multi-scale information may not be fully extracted and utilized, potentially reducing the accuracy of final recognition and affecting detection performance.

Ref [12] studied a lung CT scan image recognition method based on deep learning algorithms. It constructed a malignant tumour recognition model through deep learning, created a training set for training, and trained the global recognition model using block chain technology and joint learning algorithms. By normalizing the features of different CT scan images and incorporating the CapsNets method to classify malignant tumours, this method had been proven effective in classifying and recognizing CT images through experiments. This method integrated CT images transmitted by different CT devices. Although it can improve the accuracy of classification recognition to a certain extent, it also increased the false detection rate with increased data. This was because that the CT images from different devices and scanning conditions introduced more heterogeneity as the data

grows, which leads to poor performance in processing certain types of images and increased the false detection rate. There was still room for improvement in practical applications.

Reference [13] proposed the construction of a YOLOv5x deep learning network model based on SPECT full-body skull scanning. The training and validation set data were enhanced and input into the YOLOv5x deep learning network for training to obtain the model. The model was evaluated based on the test set to identify skull lesions in skull scanning images, and the accuracy of this method was verified through testing. However, when processing skull scan images, the position of pixels in space had not been taken into account. Therefore, not all image features can be extracted in the recognition, leading incorrect recognition of real abnormal images. This reduces the recall rate and the F1 value.

In Ref [14], the authors proposed a 3D depth feature anomaly recognition method for CT scan images based on deep learning algorithms. Using deep learning algorithms to construct an anomaly image detection model, CT scan images were converted into videos, and a pre-trained 3D ConvNet video classification network was used as the architecture. Combined with a support vector machine recursive algorithm to remove deep features from the training set, the classifier learned to classify CT anomaly images, achieving the detection of CT scan images. However, noise and artifacts may be present in CT scan images, which can interfere with the recognition performance of deep learning algorithms. Moreover, the algorithm was too complex, and it reduced the accuracy of detection when the training data was insufficient to cover all possible abnormal situations.

Sensor information fusion is a technology that combines data from multiple sensors to provide more accurate and comprehensive information. In the field of medical imaging, this technology can be applied to various imaging modalities, including skull scanning. Different sensors can provide different information, and by fusing skull scanning image information, more comprehensive and accurate skull bone images can be obtained, thereby enabling more accurate anomaly detection.

Therefore, in order to address the shortcomings of existing skull scan image anomaly detection methods and improve the accuracy of detection, this article designs a skull scan image anomaly detection method based on multi-sensor fusion. The aim is to enhance the automation level of skull scanning image detection, promote the development and innovation of medical imaging technology, and provide better medical services for patients.

The proposed algorithm solves the certain deviation problem which is generated between multiple sensors due to noise interference in the scanning process. It uses the frequency correction factor to correct the frequency domain features of sensor signals during the acquisition of bone scan images, so as to provide reliable support for subsequent fusion.

First, domain decomposition of the image for the spatial and the transform domains is carried out by using the bilateral filter and the discrete wavelet transform. Then, low frequency fusion based on guided filtering and high frequency fusion based on multi-scale morphological gradient are used to achieve whole frequency fusion respectively, and the whole frequency components after fusion are merged back into the original spatial domain to obtain the fused reconstructed image by retaining important details. Finally, the backbone network of auto encoder-decoder structure is built to learn the complex image feature representation, and the abnormal detection model is proposed according to unsupervised deep neural network.

2. Multi sensor feature data fusion and anomaly detection in skull scanning

2.1. Signal correction for multi-sensor skull scanning image acquisition

To achieve anomaly detection in skull scanning images, it is necessary to collect skull scanning images to provide input support for detection. Skull scans are typically performed using techniques such as X-rays, CT (computed tomography), MRI (magnetic resonance imaging), or nuclear medicine [15]. The application of multi-sensor fusion in skull scanning image acquisition results in fused data containing richer information, which helps detect image anomalies more accurately. However, during the process of skull scanning image acquisition, multi-sensor signals may be affected by the surrounding environment, potentially altering the frequency domain characteristics of each sensor signal and reducing the accuracy of skull scanning image acquisition [16].

Therefore, it is necessary to correct the frequency domain characteristics of the sensor signal. The transmission ability of sensor power is related to its amplitude frequency characteristics. Assuming that the input self-power spectrum of the skull scanning image I is $S_x(I)$ and the output self power spectrum is $S_y(I)$, the calculation formula for the output self power spectrum is:

$$S_y(I) = |E(I)|^2 \times S_x(I) \quad (1)$$

where, $E(I)$ represents the response function of signal frequency. The calculation formula for $S_x(I)$ is:

$$S_x(I) = \frac{[P_o(I)]^2}{M} \quad (2)$$

where, $P_o(I)$ represents the power spectral density of the sensor output signal at frequency o , and M represents the length of the sensor output signal.

The frequency domain correction factor of the sensor signal is represented by K , and the unilateral self-power spectrum of the received sensor signal is set to $G_y(I)$. The mean square value of the recovered sensor transmission signal is set to φ . Therefore, the mean square value of the recovered sensor transmission signal can be effectively calculated using the following formula:

$$\varphi = \frac{KS_y(I)}{N} \sum_{y=0}^N G_y(I) \quad (3)$$

where, N represents the number of sampling points of the sensor signal node.

From Eq.3, we know that the larger φ means better mean square value, indicating the better correction effect. The correction is completed when φ is greater than the preset threshold. When it fails to meet the requirements, the K is necessary adjusted to make φ meet the requirements by strengthening the adjustment of the output self-power spectrum of the signal.

At this point, the frequency correction factor can be used to modify the frequency domain characteristics of the sensor signal during the acquisition process of skull scanning image I , in order to enhance signal quality, reduce noise impact, and improve the accuracy of skull scanning image acquisition.

2.2. Dual domain decomposition of multi-sensor signals in skull scanning images

This article conducts dual-domain decomposition on skull scanning images, which divides the images into spatial and transformation domains. The spatial domain pertains to the distribution of pixel values in an image, while the transformation domain involves the mathematical transformation of an image into another domain to better analyze its features. Through dual-domain decomposition, skull scanning image fusion can extract feature information from images in different domains and merge this information according to specific fusion rules.

To effectively address the complex structures and features commonly encountered in skull scanning images, and to solve the problem of differentiating between abnormal areas and normal tissues, this paper combines bilateral filters and discrete wavelet transform to conduct dual-domain decomposition of spatial and transformation domains on multi-sensor signals in images. This process aims to extract more accurate and comprehensive feature information, aid in distinguishing between normal and abnormal areas, and establish the foundation for subsequent detection.

2.2.1 Spatial domain decomposition

A bilateral filter is a nonlinear filter that considers not only the spatial distance between pixels but also the differences in grayscale values between pixels [17]. Therefore, bilateral filters can preserve edge information while smoothing images, which is highly beneficial for spatial domain decomposition in skull scan image fusion.

This article employs a bilateral filter on the original skull scan image to decompose the spatial domain information of the skull scan image [18], which can preserve edge and texture information while smoothing the image. The calculation formula for pixel point and pixel neighbourhood in skull scanning images after bilateral filter decomposition is as follows:

$$R_{b,c} = \exp\left(-\frac{|B-C|^2}{2r\varepsilon_e^2}\right) \exp\left(-\frac{(f_b-f_c)^2}{\delta_d\sigma^2}\right) \varphi \quad (4)$$

In the formula, R represents the bilateral filter kernel function; B and C represent the change vectors of pixel point b and pixel neighborhood c ; r represents the radius of the square window; ε_e represents the parameter of kernel function space e ; f_b and f_c represent the pixel values of pixel point b and pixel neighborhood c ; δ_d represents the parameter of kernel function pixel range d ; σ^2 represents the variance of noise.

The spatial domain feature information of E pixel points is obtained using the following calculation formula:

$$F = \frac{\sum_{w=1}^W R_{b,c} f_c w}{\sum_{w=1}^W R_{b,c} w^2} \quad (5)$$

In the formula, F represents the spatial domain feature information of the pixel b output through a bilateral filter; W represents the filtering window of pixels; W represents the total number of pixel filtering windows.

The inclusion of bilateral filters in spatial domain decomposition means that, when processing skull scanning images, not only the positional relationship of pixels in space is considered, but also their similarity in pixel values is taken into account. This approach enables bilateral filters to effectively preserve edges and details while smoothing digital images, resulting in clearer and more natural processing outcomes. Consequently, this aids in enhancing the accuracy of anomaly detection in subsequent skull scan images.

2.2.2 Transform domain decomposition

In the decomposition of transformation domains, the Discrete Wavelet Transform (DWT) is a commonly used tool. The discrete wavelet transform is a time-frequency analysis method that can break down skull scanning images into a set of components with different frequencies. For skull scanning images, the discrete wavelet transform can decompose the image into low-frequency and high-frequency components [19]. The low-frequency component represents the overall trend and rough structure of the skull scanning image, usually containing the main information of the image, which generally corresponds to the overall shape and position of the lesion area. The high-frequency component represents the details and local changes of the skull scanning image, such as edges, textures, etc., generally corresponding to details such as the boundaries and morphological changes of the lesion area [20]. By applying the discrete wavelet transform to skull scanning images, low-frequency and high-frequency components can be processed separately to achieve better image fusion results. For example, while maintaining the low-frequency components, high-frequency components can be enhanced or suppressed to highlight the detailed information of the lesion area or remove noise.

Assuming the filter length is l , obtain the low-frequency sub image I and high-frequency sub image I_L of the original skull scan image I_L after being decomposed by the Haar filter. The formula is calculated as follows:

$$\begin{cases} I_L = \sum_{U \in N} FUI(h_1) \\ I_H = \sum_{U \in N} U(I - I_L)I(h_0) \end{cases} \quad (6)$$

In the formula, U represents the discrete time domain; h_1 and h_0 represent the coefficients of the low-pass (approximation) filter and the coefficients of the high pass (detail) filter, respectively.

After obtaining low-frequency sub image I_L and high-frequency sub image I_H , use two-dimensional discrete wavelet transform to further decompose the skull scan image into LL , LH , HL and HH . By repeating the one-dimensional decomposition process on the LL sub band, more layers of sub bands are obtained, achieving dual domain decomposition of skull scanning images. The calculation formula is as follows:

$$\begin{cases} I_{LL}(i, j) = I(2i-1, 2j-1) + I(2i-1, 2j) + I(2i, 2j-1) + I(2i, 2j) \\ I_{LH}(i, j) = -I(2i-1, 2j-1) - I(2i-1, 2j) + I(2i, 2j-1) + I(2i, 2j) \\ I_{HL}(i, j) = -I(2i-1, 2j-1) + I(2i-1, 2j) - I(2i, 2j-1) + I(2i, 2j) \\ I_{HH}(i, j) = I(2i-1, 2j-1) - I(2i-1, 2j) - I(2i, 2j-1) + I(2i, 2j) \end{cases} \quad (7)$$

In the formula, i and j represent the pixel values of pixel point b and pixel neighborhood c in the original skull scan image after wavelet decomposition.

Through wavelet decomposition, the original skull scan image is transformed into a series of subbands, each containing information about the image at different scales and directions. In summary, the dual-domain decomposition of skull scanning images in spatial and transformation domains has been completed, extracting more accurate and rich feature information as the basis for subsequent image fusion.

2.3 High and Low Frequency Fusion of Skull Scanning Images

Next, to enhance the accuracy of anomaly detection, building upon the dual-domain decomposition of skull scanning images mentioned earlier, high and low-frequency fusion processing of multi-sensor information in skull scanning images is conducted.

Firstly, multi-scale decomposition is performed on the original image to decompose it into components with different frequencies. Among them, the high and low frequency components contain different details of the image. Then, fusion rules are selected to handle high-frequency components, including maximum method and weighted fusion, where maximum method preserves sharper and more significant details in the images, while the weighted fusion method adjusts the contribution of different image sources to the fusion. Next, according to the selected fusion rules, the high-frequency components are fused. Finally, the fused high frequency component is reconstructed with the low frequency component (possibly from another image or after processing) to show the final fused image.

This process effectively integrates high and low-frequency information, preserves crucial details for all frequencies, and aids in improving the accuracy of subsequent image anomaly detection.

2.3.1 Low frequency fusion

Dual-domain decomposition typically divides an image into high-frequency and low-frequency parts. The low-frequency part usually contains the main structure and contour information of the image, while the high-frequency part contains the details and noise of the image. This article employs guided filtering to fuse the low-frequency part of skull scanning images, ensuring that the

fused image retains important structural information of the original image. Guided filtering is an edge-preserving filtering method that can maintain the clarity of edges while smoothing images. The use of guided filtering for low-frequency fusion of skull scanning images helps reduce possible artifacts and noise during the fusion process, improve the quality of fusion images, and ultimately enhance the accuracy of anomaly detection in skull scanning images.

Take the low-frequency sub-band $I_A(LL, LH)$ of image I_A as the input image for the guidance filter, and the low-frequency sub-band $I_P(LL, LH)$ of image I_P as the guidance image to obtain the blurred image $O_A(LL, LH)$ of $I_A(LL, LH)$; Take the low-frequency sub-band $I_P(LL, LH)$ of image I_P as the input image for the guidance filter, and the low-frequency sub-band $I_A(LL, LH)$ of image I_A as the guidance image to obtain a blurred image of $O_P(LL, LH)$. The calculation formula is as follows:

$$\begin{cases} O_A(LL, LH) = g[I_A(LL, LH), I_P(LL, LH), Q, D_1] \\ O_P(LL, LH) = g[I_P(LL, LH), I_A(LL, LH), Q, D_2] \end{cases} \quad (8)$$

where, Q represents the significant difference in the guided image determined by the window radius; D_1 and D_2 are regularization parameters in guided filtering.

The fusion coefficient of the low-frequency sub-band is determined by the improved Laplacian energy of the sharpened image, so it is necessary to first obtain the sharpened images of image I_A and image I_P , which can be obtained through simple calculations:

$$\begin{cases} M_A(LL, LH) = I_A(LL, LH) - O_A(LL, LH) \\ M_P(LL, LH) = I_P(LL, LH) - O_P(LL, LH) \end{cases} \quad (9)$$

Based on this, the improved Laplacian energy of sharpened image $M_A(LL, LH)$ and sharpened image $M_P(LL, LH)$ is determined to be $T(M_A)$ and $T(M_P)$. Combined with the fusion weight a , the final fusion coefficients I_A and I_P of the low-frequency subbands of image $V_{T(M_A)I_A}^a$ and image $V_{T(M_P)I_P}^a$ are obtained. Based on the weighted average fusion strategy, the possible artificial textures generated during the low-

frequency fusion process are further smoothed to achieve low-frequency fusion of skull scanning images. The formula has been calculated as follows:

$$I_{A,P}(L) = \frac{V_{T(M_A)I_A}^a T(M_A)(u,v) + V_{T(M_P)I_P}^a T(M_A)(u,v)}{V_{T(M_A)I_A}^a(u,v) + V_{T(M_P)I_P}^a(u,v)} \quad (10)$$

where, $I_{A,P}(L)$ represents the low-frequency fusion result of the skull scanning image; (u,v) represents the fusion area.

2.3.2 High frequency fusion

The high-frequency part usually contains detailed information of the image, such as edges, textures, etc. Morphological operations have a certain inhibitory effect on noise. High frequency fusion of skull scanning images through multi-scale morphological gradients can effectively suppress noise in the image and improve the signal-to-noise ratio while enhancing details. High frequency information contains multi-scale detail information in the image, making the fused image have higher resolution and clarity in detail representation.

Let the multi-scale morphological gradients of the q -th high-frequency sub band in the m -th layer of image I_A and image I_P be $Y_{I_A(HL,HH)}^{m,q}$ and $Y_{I_P(HL,HH)}^{m,q}$. The weighted local energy values of the two in the (u,v) -region are represented by $Y_{I_A}^n$ and $Y_{I_P}^n$, respectively. $Y_{I_A}^n(\beta)$ and $Y_{I_P}^n(\beta)$ are the initial weights of the high-frequency sub bands in image I_A and image I_P , and the final weight range for high-frequency fusion of the two can be determined. The calculation formula is as follows:

$$J^{m,q} = \begin{cases} 1, & \text{if } Y_{I_A}^n(\beta) > Y_{I_P}^n(\beta) \\ 0, & \text{otherwise} \end{cases} \quad (11)$$

Then, using multi-scale morphological gradients, the high-frequency sub bands of image I_A and image I_P are fused to obtain the fusion results $I_{A,P}^{m,q}$ of the high-frequency sub bands. The calculation formula is:

$$I_{A,P}^{m,q} = J^{m,q} \times \left(1 - \frac{J^{m,q} \times [Y_{I_A}^n(\beta) + Y_{I_P}^n(\beta)]}{Y_{I_A(HL,HH)}^{m,q}(u,v) + Y_{I_P(HL,HH)}^{m,q}(u,v)} \right) \quad (12)$$

Using guided filtering based low-frequency fusion algorithm and multi-scale morphological gradient based high-frequency fusion algorithm, respectively, after achieving high and low frequency fusion, using inverse wavelet transform, the fused low-frequency and high-

frequency components are merged back into the original spatial domain to obtain the reconstructed image after fusion. The calculation formula is as follows:

$$Z(I) = \exp\left(\frac{R \times \varepsilon_e^2}{U(u,v)[I_{A,P}(L) + I_{A,P}^{m,q}]} \right) \delta_d \quad (13)$$

2.4 Abnormal detection of skull scanning images

After image fusion, to enhance the accuracy and robustness of anomaly detection in skull scanning images, this paper utilizes a backbone network established by a deep learning auto encoder structure to learn complex image feature representations. Subsequently, it combines unsupervised deep neural networks to achieve anomaly detection in skull scanning images.

Unsupervised learning is a machine learning technique that enables models to learn inherent structures and patterns from input data, rather than relying on manually annotated labels. In skull scan image anomaly detection, unsupervised deep neural network models can learn patterns of normal and abnormal images from a large dataset of skull scan images without the need for pre-labeling which images are normal and which are abnormal.

A deep neural network (DNN) is a machine learning model that mimics human brain neural networks, with multiple hidden layers capable of learning and extracting complex features from input data. In unsupervised learning, DNNs can be trained to learn intrinsic features of input skull scan images for anomaly detection.

The structure of a skull scan image anomaly detection model constructed using unsupervised deep neural networks is shown in Figure 1:

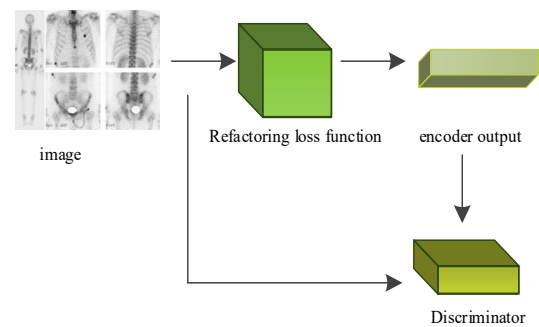


Figure 1. Schematic diagram of the structure of the anomaly detection model for skull scanning images

In the process of establishing an unsupervised deep neural network-based anomaly detection model for skull scanning images, the training of the model requires three completely different loss functions, namely:

- (1) Prioritize defining the reconstruction loss function $l_{oss(1)}$ between different images based on the degree of

difference between input image I and reconstructed image $Z(I)$, ensuring that the auto encoder in the network structure can learn the semantic information of the input skull scan image more comprehensively and accurately. The corresponding calculation formula is as follows:

$$l_{oss(1)} = X \left\| I(s) - Z(I)_s \right\|^2 \quad (14)$$

where, X represents the Manhattan distance; $I(s)$ represents the semantic information of the original skull scan image; Reconstruct the semantic information of skull scanning images using $Z(I)_s$.

(2) By setting the encoder loss function $l_{oss(2)}$ through the output hidden space z and encoder output t , it is possible to learn related content such as feature description in the hidden space through two encoders. The calculation formula is as follows:

$$l_{oss(2)} = X \left\| \chi - z(s) + z(t) \right\|^2 \quad (15)$$

where, $z(s)$ represents the semantic information contained in the output hidden space; χ represents learning information.

(3) Set the anti-loss function $l_{oss(3)}$ based on the discriminator λ of the third subnet, and the corresponding expression is as follows:

$$l_{oss(3)} = X \frac{\left\| z(s) - z(t) \right\|^2 \times \chi}{\left\| \chi - z(s) + z(t) \right\|^2} \quad (16)$$

Based on formulas (14) to (16), establish a comprehensive loss function l_{osscom} for the anomaly detection model of skull scanning images, as shown in formula (17):

$$l_{osscom} = \psi_{(1)} l_{oss(1)} + \psi_{(2)} l_{oss(2)} + \psi_{(3)} l_{oss(3)} \quad (17)$$

where, $\psi_{(1)}$, $\psi_{(2)}$, and $\psi_{(3)}$ represent adjusting parameters.

The main purpose of adjusting parameters is to effectively avoid the negative impact of the loss function on model training. It is necessary to conduct adjustment analysis based on actual situations.

In the initial stage of model training, the third discriminator corresponding to the subnet needs to be frozen, and the encoder corresponding to the first two subnets is used to search for normal and abnormal data, obtaining the optimal hidden space between the two. Furthermore, the optimal latent space is used as the basis for determining whether there are abnormalities (lesions) in the skull scan image. In the second stage of training, it is necessary to fix the parameters corresponding to the

first two encoders and use the third discriminator to locate abnormal points in the skull scanning image.

Based on the above analysis, detailed operational steps for anomaly detection in skull scanning images are provided as follows:

(1) Input the skull scanning images collected by multiple sensors, and after dual-domain decomposition and fusion, establish a set of skull scanning images θ as shown in formula (18):

$$\theta = \begin{bmatrix} o_{11} & o_{12} & o_{13} & o_{1\zeta} \\ o_{21} & o_{22} & o_{23} & o_{2\zeta} \\ \vdots & \vdots & \vdots & \vdots \\ o_{g1} & o_{g2} & o_{g3} & o_{g\zeta} \end{bmatrix} \quad (18)$$

(2) Due to the fixed position of the human skull in the collected skull scanning images, it is necessary to crop out areas that may have anomalies to improve detection accuracy.

(3) Establish the backbone network ζ of the auto encoder-decoder structure, and the corresponding calculation formula is as follows:

$$\zeta = \{\gamma_1, \gamma_2, \gamma_3, \gamma_4, \gamma_5\} \quad (19)$$

where, γ_1 represents the distance between two random encoders; γ_2 represents the true output of the encoder; γ_3 represents running time; γ_4 represents the range of values for encoder parameters; γ_5 represents the best hidden space.

(4) Establish an anomaly detection model κ for skull scanning images based on unsupervised deep neural networks, and the corresponding calculation formula is:

$$\kappa = \frac{(\zeta \times \theta) - l_{osscom}}{(z(s) - \chi) \times z(t)} \quad (20)$$

(5) Input all normal skull scan images into the model for training, obtain anomaly thresholds from all normal skull scan images, and ultimately achieve skull scan image anomaly detection.

Thus, the anomaly detection of the skull scanning image is completed through the above steps. The proposed method utilizes a frequency correction factor to modify the frequency domain characteristics of sensor signals during the acquisition process of skull scanning images, effectively reducing the impact of noise and improving data accuracy. On this basis, a combination of bilateral filters and discrete wavelet transform is used to complete the dual-domain decomposition of skull scanning images, extract more accurate and rich feature information, and help distinguish between normal and abnormal regions. Then, the low-frequency fusion algorithm based on guided filtering and the high-frequency fusion algorithm based on multi-scale

morphological gradients are used to achieve high and low-frequency fusion respectively, while retaining important details. Finally, establish a backbone network of auto encoder-decoder structure, learn complex image feature representations, and implement anomaly detection in skull scanning images based on unsupervised deep neural networks.

3. Experimental design and result analysis

3.1 Experimental Environment Setting

To investigate the practical application performance of the bone scan image anomaly detection method based on multi-sensor fusion proposed in this article, comparative tests were conducted. This study selected imaging equipment from Neusoft Group as the test subject. This imaging department encompasses various types of bone scan images from the hospital. To safeguard patient privacy, consent was obtained from all patients before collecting 600 skull scan images as the foundational image data, including images of both disease-free patients and those undergoing follow-up visits for diseases. To meet the experimental requirements, a testing environment was established for this experiment, as shown in Figure 2:



Figure 2. Schematic diagram of experimental testing environment

The environmental parameters are shown in Table 1.

Table 1 Experimental Environment Parameters

Serial Number	Project	Parameter
(1)	Visual terminal operating system	Windows 10 and above
(2)	Programming language	Python
(3)	Tool Library	Provided by third parties
(4)	Image processing tools	Opencv-contrib
(5)	Deep learning framework	Pytorch
(6)	Acceleration kits	GPU
(7)	Simulation Run Platform	MATLAB 2019a

After establishing the experimental environment, utilize the method designed in this article to train the bone scan images. The training parameters are presented in Table 2.

Table 2 Image preprocessing and training parameters

Serial Number	Project	Parameter
(1)	Training model	RTX2080ti
(2)	Learning rate	0.01
(3)	Batchsize	2.0
(4)	Resolution	1024×768
(5)	Loss degree	0.01%
(6)	Weight decay	0.0005
(7)	Periodization	100

After completing the processing, different methods are used to detect abnormal bone scan images. In order to ensure the fairness of experimental testing, the methods in reference [10] and reference [11] were used as comparison methods, and the methods in this paper were jointly tested.

3.2 Indicator Setting

Based on the above settings, firstly, to verify the effectiveness of the proposed method, skull scanning image fusion testing is conducted. The better the fusion effect, the stronger the support provided for subsequent skull scanning image anomaly detection, and the higher its reliability. Subsequently, to further validate the performance of the proposed method, the F1 score index and ROC curve index were selected, and a comparative test was carried out between the proposed method, the method in reference [10], and the method in reference [11].

Among these, the F1 score is the harmonic mean of Precision and Recall. It takes into account both accuracy and recall, making it a suitable evaluation metric for binary classification problems, particularly when categories are imbalanced. The F1 score ranges from 0 to 1, where a higher score indicates better performance of the method in detecting abnormal images in skull scanning.

True Positive Rate (TPR) and False Positive Rate (FPR) are two key indicators in the ROC curve. TPR represents the proportion of correctly predicted abnormal samples among all true abnormal samples, which is the recall rate. FPR represents the proportion of samples incorrectly predicted as abnormal among all normal samples, i.e., 1-specificity, where specificity represents the proportion of samples correctly predicted as normal among all normal samples. By adjusting the classification threshold, different TPR and FPR values can be obtained, and then the ROC curve can be plotted. The area under

the ROC curve (AUC) is an important indicator for measuring detection performance. The closer the AUC value is to 1, the higher the accuracy and effectiveness of the anomaly detection method.

3.3 Result analysis

3.3.1 Fusion effect

In the detection of anomalies in skull scanning images, the fusion effect of skull scanning images directly impacts the results of anomaly detection. Therefore, to verify the effectiveness of the proposed method, the skull scanning image fusion processing is first conducted using the proposed method. Following the design process described in this article, the skull scan images are initially fused, and the fusion effect is demonstrated by randomly selecting brain CT images and brain MRI images of the same patient, as depicted in Figure 3.

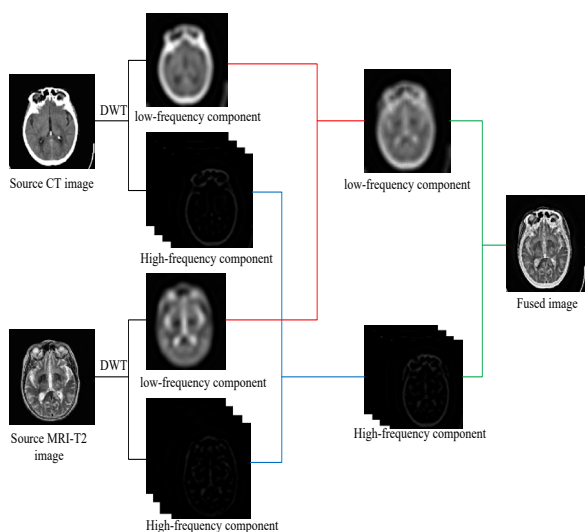


Figure 3. Skull scan image fusion effect

According to Figure 3, it is evident that the method proposed in this article can effectively fuse CT images with MRI images. The fused image exhibits clearer morphology and contours compared to the source image. While enhancing details, it effectively suppresses noise in the image and improves the signal-to-noise ratio. This indicates that the proposed method can effectively achieve fusion processing of skull scanning images, and it has a significant processing effect, providing reliable support for subsequent abnormal detection of skull scanning images.

3.3.2 F1 score comparison

Next, building upon the above tests, to verify the performance of the proposed method, a comparative test was conducted on the F1 score index between the proposed method, the method in reference [10], and the

method in reference [11]. The F1 score results of the different methods are displayed in Figure 4.

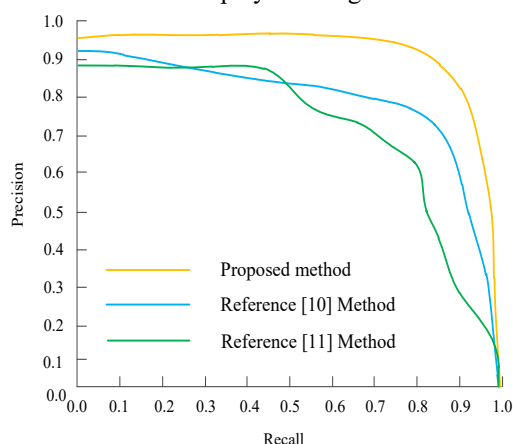


Figure 4. F1 scores of different methods

From Figure 4, it is evident that after applying the method proposed in this paper for anomaly detection in skull scanning images, the F1 score consistently outperforms the two compared methods, approaching 1. This indicates that the method proposed in this paper can accurately identify true anomalous images (with high accuracy) and cover as many actual anomalous images as possible (with high recall) when recognizing anomalous images.

However, the F1 scores of the two comparative literature methods remained consistently low, with a certain gap between them and 1. Comparing the F1 score results of the three methods reveals that our method exhibits good performance in anomaly detection tasks and can effectively recognize abnormal images from normal images. This is attributed to the method used in this article, which employs frequency correction factors to modify the frequency domain characteristics of sensor signals, enhancing signal quality, reducing noise interference, improving data accuracy, making abnormal areas more prominent in the frequency domain, and helping to identify abnormal signals more accurately. By combining bilateral filters and discrete wavelet transform, more accurate and richer feature information can be extracted from the spatial and transformation domains, aiding in better distinguishing abnormal areas from normal tissues and improving the accuracy of anomaly detection algorithms.

3.3.3 AUC Comparison

True Positive Rate (TPR) and False Positive Rate (FPR) are two key indicators in the ROC curve. By adjusting the classification threshold, different TPR and FPR values can be obtained, and then the ROC curve can be plotted. The area under the ROC curve (AUC) is an important indicator for measuring detection performance. Closer AUC to 1 means the higher accuracy and effectiveness of the anomaly detection method. The comparison of AUC using methods in References 10-11 is shown in Figure 5.

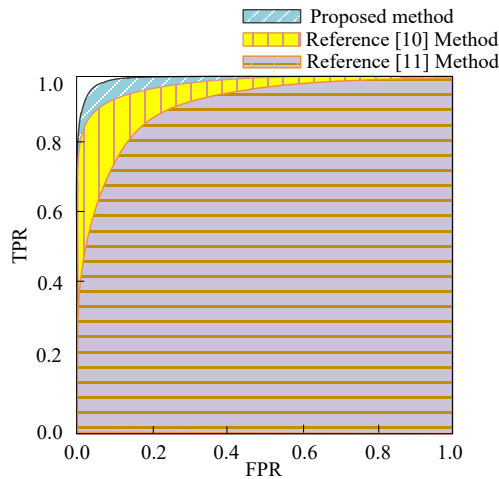


Figure 5. Comparison of AUC using different methods

According to Figure 5, it is evident that after applying the method proposed in this paper for anomaly detection in skull scanning images, the ROC curve is closest to the upper left corner. This indicates that the proposed method can accurately identify both positive and negative samples with high sensitivity and low specificity. The AUC (Area Under Curve) area under the ROC curve is relatively close to 1, signifying that the anomaly detection accuracy of this method is high and the effect is favorable.

In contrast, the ROC curves of the methods in references [10] and [11] are both lower in radian than those of the proposed method, and the AUC area is relatively small, resulting in lower accuracy in anomaly detection. Therefore, comparing the results obtained from the three methods can verify the strong reliability of our method in detecting anomalies in skull scanning images. This is because the method proposed in this article is based on a fusion algorithm of guided filtering and multi-scale morphological gradients, which effectively integrates the high and low-frequency information of the image, preserves important details, and improves the accuracy of anomaly detection. On this basis, a backbone network with an auto encoder-decoder structure is established to learn complex image feature representations, and an anomaly detection model based on unsupervised deep neural networks is established to capture the features of abnormal areas and further improve the effectiveness of anomaly detection.

4. Conclusion

In summary, to address the issues of low accuracy and poor effectiveness in anomaly detection of skull scanning images, this paper proposes a skull scanning image anomaly detection method based on multi-sensor fusion. The quality of skull scanning images and the accuracy of feature extraction have been enhanced through techniques such as frequency correction, dual domain decomposition, and high and low-frequency fusion. Simultaneously, a

skull scan image anomaly detection model was established by combining the backbone network of auto encoder structure and unsupervised deep neural network, achieving efficient and accurate anomaly detection. The experimental results demonstrate that this method exhibits high F1 score, AUC value, and sensitivity, as well as low specificity, thus confirming its effectiveness and superiority in anomaly detection of skull scanning images. This study presents a new solution for anomaly detection in skull scanning images, which holds certain theoretical significance and practical value.

Acknowledgements.

The paper was funded by Science and Technology Research Project of Jiangxi Provincial Department of Education with No.GJJ2202724.

References

- [1] Wen C, Liu S, Liu S, et al. ACSN: Attention capsule sampling network for diagnosing COVID-19 based on chest CT scans[J]. *Computers in Biology and Medicine*, 2023, 153: 106338
- [2] Sun L, Peng R. The value of integration of bone scan and targeted SPECT/CT in diagnosis of primary hyperparathyroidism with multiple bone brown tumor[J]. *Skeletal radiology*, 2023,52(12):2505-2511.
- [3] Saidi B, Fallahi B, Haghghi F, et al. Three-phase 99mTc-MDP bone scan in a case of pigment villonodular synovitis[J]. *Iranian Journal of Nuclear Medicine*, 2021(156). <https://readpaper.com/paper/3130285393>.
- [4] Zhang Y, Satapathy S C, Guttery D S, et al. Improved breast cancer classification through combining graph convolutional network and convolutional neural network[J]. *Information Processing and Management*, 2021, 58(2), 102439
- [5] Xiao Y, Xia K, Yin H, et al. AFSTGCN: prediction for multivariate time series using an adaptive fused spatial-temporal graph convolutional network[J]. *Digital Communications and Networks*, 2024, 10(2): 292-303,
- [6] Feo M D, Frantellizzi V, Rocco A D, et al. Evaluation of Bone Scan Index as a Prognostic Tool in Breast Cancer Patients with Bone Metastasis[J]. *Current radiopharmaceuticals*, 2023,16(4):284-291.
- [7] Hiddema L, Muthusami A, Brookes P, et al. 41Diagnosing Bone Metastases in Breast Cancer – CT Vs Nuclear Medicine Bone Scan[J]. *British Journal of Surgery*, 2021, 108(Supplement 2), znanb135.024.
- [8] Song L, Liu X, Chen S, et al. A deep fuzzy model for diagnosis of COVID-19 from CT images[J]. *Applied Soft Computing*, 2022, 122: 108883
- [9] Meyers J L, Cardoso H F V. Reliability of wet versus dry bone CT scan-based quantification of cortical area measurements[J]. *American Journal of Physical Anthropology*, 2021, 174(Suppl.71): 71-71.
- [10] Malloy P, Newhouse A C, Alejandro A. Espinoza Orías, et al. MRI-- and CT--based metrics for the quantification of arthroscopic bone resections in femoroacetabular impingement syndrome[J]. *Journal of Orthopaedic Research*, 2022, 40(5): 1174-1181.

- [11] Banday S A, Nahvi R, Mir A H, et al. Ground glass opacity detection and segmentation using CT images: an image statistics framework[J]. *IET image processing*, 2022, 16(9): 2432-2445.
- [12] Heidari A, Javaheri D, Toumaj S, et al. A new lung cancer detection method based on the chest CT images using Federated Learning and blockchain systems[J]. *Artificial intelligence in medicine*, 2023, 141(7): 1.
- [13] Li Z, Zhao Z, Lian S. YOLOv5x deep learning network model based on SPECT whole body bone scanning for diagnosing benign and malignant bone lesions[J]. *Chinese Journal of Medical Imaging Technology*, 2023, 39(12): 1867-1871.
- [14] Chen J, Wee L, Dekker A, et al. Using 3D deep features from CT scans for cancer prognosis based on a video classification model: A multi-dataset feasibility study[J]. *Medical physics*, 2023, 50(7): 4220-4233.
- [15] Cerci J J, Fanti S, Lobato E E et al. Diagnostic Performance and Clinical Impact of Ga-68-PSMA-11 PET/CT Imaging in Early Relapsed Prostate Cancer After Radical Therapy: A Prospective Multicenter Study (IAEA-PSMA Study)[J]. *The Journal of Nuclear Medicine*, 2022, 63(2): 240-247.
- [16] Rashid R, Zhang E, Abdi A. Some measured frequency domain characteristics of the underwater vector and scalar acoustic field components with applications to communication receivers[J]. *The Journal of the Acoustical Society of America*, 2021, 150(4): A155.
- [17] Liu X, Hou S, Liu S, et al. Attention-based Multimodal Glioma Segmentation with Multi-attention Layers for Small-intensity Dissimilarity[J]. *Journal of King Saud University - Computer and Information Sciences*, 2023, 35: 183-195
- [18] Manikandan L C, Selvakumar R K, Nair S A H, et al. Hardware implementation of fast bilateral filter and canny edge detector using Raspberry Pi for telemedicine applications[J]. *Journal of Ambient Intelligence and Humanized Computing*, 2021, 12(5): 4689-4695.
- [19] Geetha V, Anbumani V, Murugesan G, et al. Hybrid optimal algorithm-based 2D discrete wavelet transform for image compression using fractional KCA[J]. *Multimedia Systems*, 2020, 26(8): 1-16.
- [20] Han H, Wang X. Fast Multi-Sensor Information Fusion Based on Deep Hybrid Convolution[J]. *Computer Simulation*, 2022, 39(05): 288-291+298.